Iran. J. Radiat. Res., 2012; 9(4): 209-219

FDG-PET/MRI fused data sets for the detection of liver metastases in patients undergoing systemic anticancer treatment

T.A. Heusner[1*], C. Mikat[2], S. Hahn[2], J. Altenbernd[2], A. Stahl[3], A. Bockisch[3], M. Forsting[2], G. Antoch[1]

[1]University of Dusseldorf, Medical Faculty, Department of Diagnostic and Interventional Radiology, D-40225 Dusseldorf, Germany
[2]University of Duisburg-Essen, Medical Faculty, Department of Diagnostic and Interventional Radiology and Neuroradiology, D-45147 Essen, Germany
[3]University of Duisburg- Essen, Medical Faculty, Department of Nuclear Medicine, D-45147 Essen, Germany

Background: To retrospectively describe imaging characteristics of liver metastases on fused FDG-PET/MRI data sets and to compare the diagnostic accuracy of MRI and fused FDG-PET/MRI data sets for the detection of liver metastases in patients undergoing systemic anticancer treatment. ***Materials and Methods:*** 43 oncological patients (mean age: 56+/- 11 years) were investigated by FDG-PET/CT and liver MRI. FDG-PET data from PET/CT scans were fused with MRI. 556 lesions were evaluated. 5 different evaluation algorithms were used for FDG-PET/MRI evaluation. The sensitivity, specifity, PPV, NPV and accuracy of MRI and FDG-PET/MRI data for the detection of liver metastases were calculated. A mean follow-up of 647 days served as reference standard. McNemar's test was used to test for statistically significant differences between MRI and FDG-PET/MRI ($p<0.5$). ***Results:*** The sensitivity, specificity, PPV, NPV and accuracy of MRI for the detection of liver metastases were 86%, 81%, 97%, 47%, and 85% and 50%, 100%, 100%, 22%, and 56%, for FDG-PET/MRI. FDG-PET/MRI was significantly less accurate than MRI alone ($p<.001$). ***Conclusion:*** In opposite to patients before systemic anticancer therapy the fusion of FDG-PET data with liver MRI cannot be recommended for the detection of liver metastases in patients undergoing systemic oncological therapy. **Iran. J. Radiat. Res., 2012; 9(4): 209-219**

Keywords: *PET/MRI, PET/CT, liver MRI, liver metastases, hybrid imaging.*

INTRODUCTION

Cancer diseases represent a major public health problem in western countries [1, 2]. Currently one out of four deaths in the United States is due to cancer [2]. Once cancer has been diagnosed the stage of the disease at the time of diagnosis constitutes the basis in determining appropriate oncological treatment strategies. The knowledge of the exact tumor stage is essential to choose stage-adapted therapeutic strategies in order to increase the chance for and the duration of survival [1]. In this setting the liver is of special interest as it represents an organ frequently harbouring distant metastases. Due to the importance of this organ for staging procedures an imaging method as accurate as possible has to be aimed for. For this purpose several imaging modalities such as computed tomography (CT), magnetic resonance imaging (MRI), positron emission tomography (PET), and positron emission tomography/computed tomography (PET/CT) are available in clinical routine [3-7]. CT and MRI as stand-alone modalities predominantly offer morphological information with functional information (such as perfusion and diffusion imaging) only available to a limited level in clinical routine [8, 9]. When comparing CT and MRI for imaging the liver there is an obvious advantage of MRI over CT: MRI is able to provide a superior soft tissue contrast resulting in a higher accuracy for

Corresponding author:
Dr. Till A. Heusner,
University of Dusseldorf, Medical Faculty, Department of Diagnostic and Interventional Radiology, D-40225 Dusseldorf, Germany.
Fax: *+49 211 8111645*
E-mail: *Heusner@med.uni-duesseldorf.de*

the detection of liver metastases [10]. In contrast to morphological imaging modalities PET mainly offers functional information, with only limited morphological data based on its poor spatial resolution. To overcome the limitations of separate morphological and functional imaging methods hybrid PET/CT machines have been developed and established in clinical routine [5, 11-13]. Several studies have documented a superior diagnostic accuracy of combined PET/CT over separate PET or CT imaging alone for staging purposes [5, 14-16]. Combined PET/MRI machines were available for cerebral applications only for a longer time; just now first whole-body PET/MRI scanners are introduced into clinical routine. It is obvious that more and more combined whole-body PET/MRI scanners will find their way into clinical practice in the near future [17-19]. Potential indications in which PET/MRI may be of higher diagnostic accuracy than PET/CT may be those in which MRI has been found to be more accurate than CT; these indications may include tumors where imaging profits from the high soft-tissue contrast of MRI, such as liver metastases. However, till today, there has been only little experience on the evaluation of metastases with PET/MRI [20]. For patients with suspected liver metastases before therapy it has been recently shown that software-based fused 2-deoxy-2-[^{18}F]-fluoro-D-glucose (FDG)-PET/MRI data sets (using FDG-PET data that were extracted from FDG-PET/CT data sets) are of higher diagnostic value than FDG-PET/CT [21]. Data concerning the diagnostic value of fused FDG-PET/MRI data sets for the detection of liver metastases in patients under systemic treatment however are still lacking. Therefore the aim of this retrospective study was to evaluate the diagnostic accuracy of FDG-PET/MRI data sets fused on a software-basis for the detection of liver metastases in patients undergoing systemic anticancer therapy and to compare these imaging results with MRI alone.

MATERIALS AND METHODS

Patients

43 patients (mean age, 56.1 years (y); range, 35.3-71.3 y; standard deviation (SD), 11.4 y, 24 men, 19 women)) with different histopathologically proven malignancies and liver metastases either verified on MRI or FDG-PET(/CT) were included in this retrospective study. For a detailed summary concerning the primary tumor entities please see table 1. All patients underwent FDG-PET/CT scans as well as MRI of the liver in clinical routine for restaging purposes. Patients were consecutive concerning the following inclusion criteria:

- histopathologically proven malignancy
- malignancy with established FDG-PET positivity
- liver metastases proven by prior cross-sectional imaging
- MRI and FDG-PET/CT data sets of the liver acquired a maximum of 6 weeks apart
- currently undergoing systemic therapy
- follow-up cross-sectional liver imaging available as reference standard.

Table 1. Histopathology of malignancies in the study population.

Primary lesion	n	%
bronchial carcinoma	6*	14*
gastric cancer	1	2
colorectal cancer	14	33
malignant melanoma (skin)	1	2
neuroendocrine tumor	2	5
breast cancer	9	21
head and neck cancer	2	5
genitourinary cancer	4	9
soft-tissue sarcoma	1	2
thyroid cancer	1	2
cancer of unknown primary	2	5
total	**43**	**100**

*: 1 female patient suffered from a histopathologically proven bronchial carcinoma, as well as breast cancer and an oropharyngeal carcinoma in medical anamnesis.

The mean time distance between in between MRI and PET/CT was 6 days (d) (range, 0-42 d; SD, 18 d). All patients signed an informed consent that detailed the use of intravenous FDG, CT contrast material, and MR contrast material and rare potential side effects. The study was performed according to the guidelines of the local ethics committee.

FDG-PET

For later fusion with MRI images liver PET data sets from whole-body FDG-PET/CT investigations were used. All patients were instructed to fast at least six hours before FDG-PET/CT imaging. One hour before the examination, all patients drank 1000 ml of a water-equivalent oral contrast agent [22]. Before intravenous tracer injection, blood glucose levels were ensured to be below 150 mg/dl. FDG-PET/CT investigations were performed using a biograph™ PET/CT (Siemens Medical Solutions, Hoffman Estates, Illinois, USA) composed of a dual-slice CT scanner (Somatom Emotion™, Siemens Medical Solutions, Forchheim, Germany) and a full-ring PET working with bismuth germinate crystals (ECAT HR+™, Siemens Molecular Imaging, Hoffman Estates, Illinois, USA). CT was performed first, followed by PET. Whole-body CT (130 mAs, 130 kV, slice thickness: 5 mm, table feed: 8 mm, incremental reconstruction: 2.4 mm) covered a region ranging from the skull base to the upper thighs. 140 ml of an iodinated contrast material (Ultravist 300™, Schering AG, Berlin, Germany) were applied intravenously with an automated injector (XD 5500™, Ulrich Medical Systems, Ulm, Germany) using a flow rate of 3 ml/s for the first 90 ml and 1.5 ml/s for the following 50 ml. The start delay was 50 s. A limited breath-hold technique was used to avoid motion-induced artifacts within the liver [23]. The acquisition of the PET data started 60 minutes after intravenous injection of FDG. The PET system worked with an axial field of view of 15.5 cm/bed position and an in-plane spatial resolution of 4.6 mm. PET was acquired in a 3 D mode. The emission time was adapted to the patients' body weight: < 65 kg – 4 min/bed position, 65-85 kg – 5 min/bed position, > 85 kg – 6 min/bed position. Iterative algorithms (FORE and AWOSEM, non-linear, 2 iterations, 8 subsets) were used for reconstruction of the PET images. Data were filtered (FWHM 5.0 mm) and corrected for scatter. Image reconstruction was performed with and without PET attenuation correction. CT data were used for attenuation correction of the PET data.

MRI

All liver MR examinations were performed on a current generation 1.5T scanner (Magnetom Avanto™, Siemens Medical Solutions, Erlangen, Germany, or Magnetom Espree™, Siemens Medical Solutions, Erlangen, Germany). A phased-array surface coil was used for signal reception covering the upper abdomen. Routine imaging consisted of pre-contrast MR sequences in the axial plane including a pre-contrast T1-weighted (T1w) sequence acquired as breath-hold spoiled gradient dual-echo in- and out-of-phase (SGE) sequence (TR 117 msec, TE 2.22 msec, flip angle 70°, slice thickness (ST) 7 mm, slice spacing (SP) 8.4 mm, matrix size 256×34) and a fat-saturated T2-weighted (T2w) half-Fourier acquisition single-shot turbo spin echo (HASTE) sequence (TR 1000 msec, TE 107 msec, flip angle 150°, ST 5 mm, SP 6.5 mm, matrix size 320×176). Subsequently a T2w fat-saturated turbo spin echo sequence (TR 4450 msec, TE 84 msec, flip angle 150°, ST 7 mm, SP 8.4 mm, matrix size 256×154) in the axial plane and a T2w true fast imaging with steady state precession (TrueFISP) sequence (TR 3.61 msec, TE 1.81 msec, flip angle 80°, ST 5 mm, SP 6.5 mm, matrix size 256×156) in the coronal plane were added. Before contrast material administration an axial volume interpolated breath-hold examination (VIBE) sequence (TR 4.11 msec, TE 1.67 msec, flip angle 12°, ST 3.5

mm, matrix size 512×166) was conducted during which the patient was instructed to hold his breath in inspiration. Gadolinium was administered intravenously as a power-injected (Spectris Solaris™, Medrad, Pittsburgh, PA, USA) bolus of a gadolinium chelate (0.1 mmol/kg Gadovist™, Bayer-Schering Pharma, Berlin, Germany or 0.1 mmol/kg Dotarem™; Guerbet, Roissy, France) at 2 mL/s followed by a saline flush in all patients. 3 contrast-enhanced VIBE sequences were added (parameters see above). VIBE sequences were performed 22 sec (arterial phase), 32 sec (portalvenous phase) and 42 sec (venous phase) after contrast material administration. At last one fat-saturated T1w fast low angle shot (FLASH) 2D sequence in axial direction (TR 120 msec, TE 2.47 msec, flip angle 70°, ST 7 mm, SP 8.4 mm, matrix size 320×168) and one in coronal direction (TR 121 msec, TE 2.44 msec, flip angle 70°, ST 5 mm, SP 6.5 mm, matrix size 256×146) were added.

FDG-PET/MRI

FDG-PET/CT data sets and the liver MRI data sets were transferred to a picture archiving and communication system (PACS, General Electrics Healthcare, General Electrics Munich, Germany). From each patient, the attenuation-corrected axial FDG-PET images as well as the axial venous VIBE sequence were transferred to a TrueD™ fusion workstation (Siemens, Malvern, USA) via the hospital network. The MRI set was treated as the reference volume, whereas the FDG-PET data set was treated as the volume to be registered. Data sets were semiautomatically fused by using the "landmark matching" tool of the TrueD™ workstation. Corresponding landmarks in both data sets were defined with the following images displayed at the same time: venous VIBE MRI sequence, FDG-PET, and FDG-PET/MRI in an axial, coronal, and sagittal view each. We defined absolute and relative landmarks. Absolute landmarks were represented by reproducible anatomic structures such as for example the spine or the apex of the heart, relative landmarks were represented by anatomic structures relative to an absolute landmark, for example the liver margins (e.g. the lower edge of liver segment 6) or skin boundaries. Once a landmark was chosen, the pixel was marked in the MR mammography and PET data set and a sequential number was assigned. The landmark matching tool fused both data sets semiautomatically in all 3 planes considering all determined landmarks. Each fused FDG-PET/MRI series was saved as a separate DICOM file.

Image analysis

MRI images were evaluated in the axial plane, fused FDG-PET/MRI images were evaluated in the axial, coronal and sagittal plane. On MRI and FDG-data sets both a qualitative as well as a quantitative evaluation were performed as follows:

Qualitative MRI evaluation:

- Evaluation of the lesions visibility: differentiation into "visible" and "invisible" lesions (a lesion that was detectable on FDG-PET may not have had a correlate on MRI - "invisible" lesion)
- Evaluation of the lesions signal intensity: differentiation into hypointense, isointense, and hyperintense lesions on T1w and T2w images each
- Evaluation of the enhancement on contrast-enhanced VIBE sequences according to a 4-point scale (no, faint, moderate, or strong uptake)

Quantitative MRI evaluation:

- Evaluation of the lesions greatest axial diameter in millimeter (mm)

Qualitative FDG-PET evaluation:

- Evaluation of the lesion´s FDG uptake compared to unaffected liver tissue (differentiation between focally elevated uptake or no focally elevated uptake)

Semi-quantitative FDG-PET evaluation:

- Measurement of the maximum standardized uptake value (SUVmax) by drawing a circle covering the lesion

as the region of interest (ROI) using the toolbar of the AW Suite™ Volume viewer plus™ software (General Electrics Healthcare, General Electrics, München, Germany). The SUV_{max} was calculated according to the following equation:

$$SUV\ \max = \frac{\text{measured maximum activity concentration [MBq/ml]}}{\text{injected dose [MBq] per body weight [g]}}$$

Analysis of all data sets was performed by two radiologists and one nuclear medicine physician. Diagnoses were made in consensus. All images were evaluated on a PACS workstation (General Electrics Healthcare, General Electrics München, Germany) as well as on the TrueD™ fusion workstation (Siemens, Malvern, USA).

Statistical Validation / Lesion Classification

After lesion evaluation we divided the lesions into benign hepatic lesions and hepatic metastases according to their appearance on MRI and FDG-PET/MRI: A metastasis on MRI was defined as a lesion showing a hypointense signal on T1, a slightly hyperintense signal on T2 and at least a faint contrast material uptake. On fused FDG-PET/MRI 5 different algorithms were applied to test for metastases:

1. Metastasis defined as lesion of any size with hypointense signal on T1w images, hyperintense signal on T2w images, at least faint MR contrast material uptake, focally elevated FDG uptake, SUV_{max} of at least 6.
2. Metastasis defined as lesion of any size with hypointense signal on T1w images, hyperintense signal on T2w images, at least faint MR contrast material uptake, focally elevated FDG uptake compared to surrounding unremarkable liver tissue (irrespective of the absolute SUV_{max}).
3. Metastasis defined as lesion with hypointense signal on T1w images, hyperintense signal on T2w images, at least faint MR contrast material uptake, focally elevated FDG uptake (irresepective of the absolute SUV max), lesion size ≥ 5 mm.
4. Metastasis defined as lesion with hypointense signal on T1w images, hyperintense signal on T2w images, at least faint MR contrast material uptake, focally elevated FDG uptake (irrespective of the absolute SUV max), lesion size ≥ 10 mm.
5. Metastasis defined as lesion with hypointense signal on T1w images, hyperintense signal on T2w images, at least faint MR contrast material uptake, focally elevated FDG uptake (irrespective of the absolute SUV max), lesion size ≥ 15 mm.

Subsequently the findings were compared to the reference standard and the sensitivity, specificity, the positive predictive value (PPV), the negative predictive value (NPV) as well as the accuracy were determined for MRI and FDG-PET/MRI. Differences in the accuracy of both data sets (MRI and FDG-PET/MRI) was tested for statistical significance by McNemar's test ($p<0.5$).

Standard of reference

Cross-sectional imaging follow-up data with a mean duration of 647 days (range, 56 -1674 d; SD, 490 d) served as the standard of reference in all patients. Cross-sectional imaging follow-up consisted of CT, FDG-PET/CT, and MRI.

RESULTS

Overall 556 hepatic lesions were evaluated in 43 patients. According to the standard of reference 483 lesions (87%) turned out to be metastases and 73 lesions were benign lesions (13%).

Overall lesion appearance on MRI

The vast majority of the lesions (n=552, 99%) was detectable on MRI; 4 lesions (1%) with focally increased FDG uptake on PET

had no correlate on MRI. On non-enhanced T1w images 549 of the 552 visible lesions (99%) turned out to be hypointense whereas 3 lesions (1%) were hyperintense. On T2w images 537 lesions (97%) showed a hyperintense signal and 14 lesions a hypointense signal (3%). 1 lesion was not identifiable on T2w images. 112 lesions (20%) showed no contrast material uptake on MRI, 388 lesions (70%) had a faint uptake, 41 lesions (7%) had an uptake classified as moderate, and 11 lesions (3%) had a strong contrast material uptake. Lesions had a mean axial diameter of 14 mm (range, 2- 80 mm; SD, 9.8 mm).

Overall lesion appearance on FDG-PET

On FDG-PET images, 238 lesions (43%) showed a clearly visible, focally elevated uptake compared to unaffected liver tissue whereas 318 lesions (57%) showed equivocal uptake compared to surrounding liver tissue. The mean SUVmax of all lesions was 6.6 (range, 0.9-18.7; SD, 3.9). The mean SUVmax of the lesions showing focally elevated FDG uptake was 10.2 (range, 3.9-18.7; SD, 2.9); the mean SUVmax of the lesions not showing focally elevated FDG uptake was 3.9 (range, 0.9-10.4; SD, 1.8).

Appearance of benign liver lesions and liver metastases on MRI

MRI was compared with the reference standard. Nearly all lesions defined as metastases based on the reference standard showed a hypointense signal on non-enhanced T1w images and a hyperintense signal on T2w images (99% both for T1 and T2), whereas lesions defined as benign by the reference standard showed the same signal intensity (hypointense on T1w images and hyperintense on T2w images) in 93% and 77% of cases respectively. 87% of the metastases had at least a faint contrast material uptake on the VIBE sequences compared. Lesions defined as benign according to the reference standard demonstrated contrast material uptake in only 28%. For a detailed summary please see table 2.

Table 2. Lesion's characteristics (size, MR signal intensity, rim contrast enhancement).

	Metastases	Benign findings
lesion´s size (mm)		
mean	14	19
min	1	3
max	73	80
SD	8.9	17.7
p	0.398	
signal intensity on T1w images (n (%))		
not visible	0 (0%)	4 (6%)
hypointense	481 (99%)	68 (93%)
isointense	0 (0%)	0 (0%)
hyperintense	2 (1%)	1 (1%)
signal intensity on T2w images (n (%))		
not visible	1 (0.2%)	4 (5%)
hypointense	1 (0.2%)	13 (18%)
isointense	0 (0%)	0 (0%)
hyperintense	481 (99.6%)	56 (77%)
rim contrast enhancement		
lacking	64 (13.3%)	52 (72%)
faint	371 (77%)	17 (23%)
moderate	38 (8%)	3 (4%)
strong	10 (2%)	1 (1%)

Appearance of benign liver lesions and liver metastases on FDG-PET

On qualitative PET evaluation approximately half of the lesions defined as metastases according to the reference standard showed a focally elevated FDG uptake compared to surrounding liver tissue (48%), the others (52%) did not show any focally elevated FDG uptake. The SUVmax of hepatic metastases was significantly higher than the SUVmax of benign lesions (7.1 versus 3.2, p<0.001). For a detailed summary please see table 3.

Diagnostic accuracy of MRI for the detection of liver metastases

MRI alone had 68 false negative (fn), 14 false positive (fp), 59 true negative (tn), and 415 true positive (tp) findings; correspondingly the sensitivity, specificity, PPV, NPV and accuracy was 86%, 81%, 97%, 47%, and 85%. For a detailed summary please see table 4.

Table 3. Lesion's qualitative and quantitative FDG uptake.

	metastases	benign findings
qualitative FDG uptake (n (%))		
focal FDG uptake compared to surrounding liver uptake	234 (48%)	4 (6%)
no focal FDG uptake compared to surrounding liver uptake	249 (52%)	69 (94%)
quantitative FDG uptake (SUVmax)		
mean	7.1	3.2
min	0.9	1
max	18.7	5.7
SD	3.89	1.1
p	<0.001	

Table 4. Diagnostic accuracy of MRI and FDG-PET/MRI using different metastases' definitions.

modality	**MRI**	**FDG-PET/ MRI[1]**	**FDG-PET/ MRI[2]**	**FDG-PET/ MRI[2]**	**FDG-PET/ MRI[2]**	**FDG-PET/ MRI[2]**
lesion diameter	all	all	all	≥ 5 mm	≥ 10 mm	≥ 15 mm
number of lesions	556	556	556	514	365	193
metastases (n)	483	483	483	452	324	165
benign lesions (n)	73	73	73	62	41	28
tp	415	267	233	225	163	75
tn	59	75	73	62	41	28
fp	14	0	0	0	0	0
fn	68	214	250	227	161	90
sensitivity	86%	45%	48%	50%	50%	46%
specificity	81%	100%	100%	100%	100%	100%
PPV	97%	100%	100%	100%	100%	100%
NPV	47%	22%	23%	22%	20%	24%
accuracy	85%	52%	55%	56%	56%	53%

[1] Definition of a metastasis on FDG-PET/MRI: hypointense signal on T1w images, hyperintense signal on T2w images, contrast material uptake visible, SUVmax 6 or more.

Diagnostic accuracy of fused FDG-PET/MRI data sets for the detection of liver metastases

Fused FDG-PET/MRI data sets were reviewed using 5 different evaluation algorithms. Algorithms were different from each other concerning the appearance of the lesions on FDG-PET and were scaled according to the lesions´ size:

1. Applying evaluation algorithm 1 FDG-PET/MRI had 265 fn, 0 fp, 73 tn, and 218 tp findings; the sensitivity, specificity, PPV, NPV and accuracy were 45%, 100%, 100%, 22%, and 52% (figure 1, 2). In this scenario FDG-PET/MRI was significantly less accurate than MRI alone for the detection of liver metastases (p<.001).
2. Applying evaluation algorithm 2 FDG-PET/MRI data sets had 250 fn, 0 fp, 73 tn, and 233 tp findings; the sensitivity, specificity, PPV, NPV and accuracy was 48%, 100%, 100%, 23%, and 55%. FDG-PET/MRI was significantly less accurate than MRI alone for the detection of liver metastases (p<.001).
3. Applying evaluation algorithm 3 FDG-PET/MRI data sets had 227 fn, 0 fp,62 tn, and 225 tp findings; the sensitivity, specificity, PPV, NPV and accuracy were 50%, 100%, 100%, 22%, and 56%. FDG-PET/MRI was significantly less accurate than MRI alone for the detection of liver metastases (p<.001)
4. Applying evaluation algorithm 4 FDG-PET/MRI data sets had 161 fn, 0 fp,41 tn, and 163 tp findings; the sensitivity, specificity, PPV, NPV and accuracy were 50%, 100%, 100%, 20%, and 56%. FDG-PET/MRI was significantly less accurate than MRI alone for the detection of liver metastases (p<.001).

Applying evaluation algorithm 5 FDG-PET/MRI data sets had 90 fn, 0 fp, 28 tn, and 75 tp findings; the sensitivity, specificity, PPV, NPV and accuracy were 46%, 100%, 100%, 24%, and 53%. FDG-PET/MRI was significantly less accurate than MRI alone for the detection of liver metastases (p<.001). For a detailed summary please see table 4.

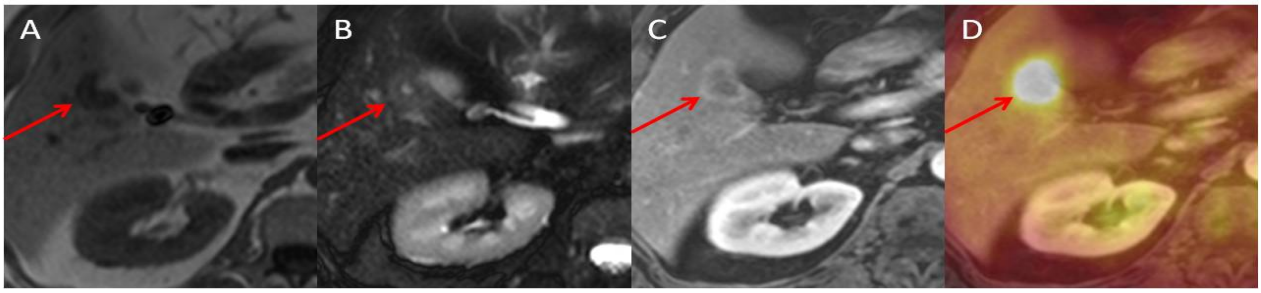

Figure 1. True positive lesion on MRI as well as on FDG-PET/MRI: 64 year-old male patient with a rectal cancer liver metastasis located in Coinaud's segment 6 showing the typical signal intensity on MRI (hypointense on T1w images (A), hyperintense on T2w images (B), rim enhancement after i.v. gadolinium administration (VIBE sequence, C)) as well as focal FDG uptake on FDG-PET/MRI (D).

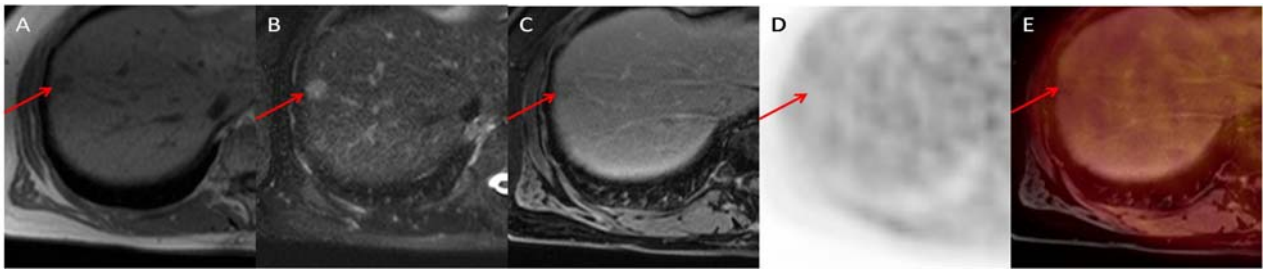

Figure 2. True positive lesion on MRI / false negative lesion on FDG-PET/MRI: 68 year-old male suffering from medullar cancer of the thyroid gland. The patient was under systemic anticancer therapy at time of imaging. On T1w images the liver metastasis in Coinaud´s segments 8 showed a hypointense signal (A) and on T2w images a hyperintense signal (B). The metastasis had a faint contrast material uptake in the VIBE sequence (C) but did not show any elevated FDG uptake on fused FDG-PET (D) and FDG-PET-PET/MRI (E), so following the evaluation algorithm in use the lesion was falsely rated as negative for malignancy.

DISCUSSION

Just now combined whole-body PET/MRI scanners starting to find their way into clinical practice [17-19]; nowadays only a few scanners are installed worldwide, so these scanners are accessible only to a limited number of patients. On the other hand MRI and PET/CT scanners are much more widespread. FDG-PET data can be extracted from the FDG-PET/CT scans and fused with MRI on a software-basis. PET/MRI data (either fused on a software or hardware basis) may have the ability to further increase the diagnostic accuracy over PET/CT especially when evaluating organs where imaging benefits from the high soft-tissue contrast of MRI. The liver is one of these organs. For patients with suspected liver metastases before therapy Donati and colleagues showed that software-based fused data sets offer a higher diagnostic accuracy for the detection of liver metastases than FDG-PET/CT [21]. In opposite to these results our results emphasize that in the setting of patients undergoing anticancer therapy the evaluation of MRI data reaches a significantly higher accuracy (85% versus 56%) and sensitivity (86% versus 50%) for the detection of liver metastases than FDG-PET/MRI. In other words, the addition of functional FDG-PET data to liver MRI substantially deteriorated the accuracy of liver MRI. This phenomenon must be attributed to the patient population (systemic or local anticancer therapy). It has been shown previously, that systemic treatment results in a decrease in FDG-uptake in malignant lesions in the case of therapy response [24]. Thus, only 48% of hepatic metastases demonstrated focal FDG uptake in this study. Another factor may be a physiologically strong FDG-uptake of normal liver parenchyma [25]. Even though the SUVmax of metastases was significantly higher than the SUVmax of benign lesions many lesions embedded in physiological liver tissue did not show definite elevated FDG uptake.

Another explanation for the poor performance of fused FDG-PET/MR images may be the limited spatial resolution of the PET system: in consequence elevated FDG uptake of small lesions with a diameter of less than 5 mm may not be detected. However, this technical limitation seems to be only of limited effect in the current study as the sensitivity of FDG-PET/MRI for the detection of metastases larger than 5 mm was only slightly better. Thus, treatment-associated PET-negativity must be considered the main factor for the poor performance of PET/MR.

On the other hand FDG-PET/MRI did not have false positive result, in contrast to MRI which detected 14 false positive lesions. This resulted in specificity and a PPV of 100% each with FDG-PET/MRI. Differentiation of MR-indeterminate lesions with FDG-PET/MRI may be a potential indication in this clinical scenario.

Though our results demonstrated only a moderate accuracy for the detection of liver metastases by FDG-PET/MRI the use of fused FDG-PET and MRI datasets may have diagnostic impact when evaluating response to systemic therapies: FDG-PET is known to early detect a response to systemic therapy when morphological parameters are still unchanged [26-28]. However, in this setting a pretreatment scan should be performed to demonstrate FDG-uptake of the tumor and to have a baseline with which follow-up imaging can be compared.

This study has some limitations: As this was a retrospective study MRI and FDG-PET data were acquired for clinical patient work-up but not specifically for software-based PET/MRI image fusion. As a consequence FDG-PET and MRI data sets were acquired in different breathing positions: PET data were acquired in shallow breathing whereas MRI was acquired in inspiration. This difference in breathing positions may have affected the accuracy of image fusion. Additionally, in some patients with time interval in between

PET and MRI was longer than 6 days. Within this period morphological and functional characteristics of metastases may have changed making accurate image fusion difficult. A further limitation is the standard of reference: Optimally, histopathology would be available as a reference standard. However, in this patient population a large number of patients suffered from disseminated metastases in the liver, thus histopathology cannot be considered a practical, nor ethically acceptable approach. Therefore, imaging follow-up was chosen as a reference standard.

In conclusion in patients with current anticancer therapy MRI alone is of higher accuracy than fused FDG-PET/MRI data sets for the detection of liver metastases. The results indicate that the addition of FDG-PET information to MRI does not add information concerning the detection of metastases in this specific patient population. These results are in opposite to the results in patient populations before systemic therapy as shown before [21]. Based on these results we recommend either to investigate patients by using fused FDG-PET/MRI data sets from the beginning (both before and during their further disease course) or to stay with MRI follow-up if initial FDG-PET data is lacking.

ACKNOWLEDGEMENT

We thank Slvco Maric, RT, and Anton Quinsten, RT for performing the FDG-PET/CT and MRI scans.

REFERENCES

1. Edge SBB DR, Compton CC, Fritz AG, Greene FL, Trotti A (2010) AJCC Cancer Staging Manual. American Joint Committee on Cancer.
2. Jemal A, Siegel R, Ward E, Hao Y, Xu J, Thun MJ (2009) Cancer statistics. *CA Cancer J Clin,* ***59****:225-249.*
3.Stahl A, Wieder H, Wester HJ, Piert M, Lordick F, Ott K, *et al.* (2004) PET/CT molecular imaging in abdominal oncology. *Abdom Imaging,* ***29:*** *388-397.*
4. Antoch G, Vogt FM, Bockisch A, Ruehm SG (2004) [Whole-body tumor staging: MRI or FDG-PET/CT?]. *Radiologe,* ***44:*** *882-888.*
5. Antoch G, Vogt FM, Freudenberg LS, Nazaradeh F, Goehde SC, Barkhausen J, *et al.* (2003) Whole-body dual-modality PET/CT and whole-body MRI for tumor staging in oncology. *Jama,* ***290:*** *3199-3206.*
6. Heusner T, Golitz P, Hamami M, Eberhardt W, Esser S, Forsting M, *et al.* (2009) "One-stop-shop" staging: Should we prefer FDG-PET/CT or MRI for the detection of bone metastases? *Eur J Radiol,* ***78:*** *430-435.*
7. Heusner TA, Kuemmel S, Umutlu L, Koeninger A, Freudenberg LS, Hauth EA, *et al.* (2008) Breast cancer staging in a single session: whole-body PET/CT mammography. *J Nucl Med,* ***49:*** *1215-1222.*
8. Dugdale PE and Miles KA (1999) Hepatic metastases: the value of quantitative assessment of contrast enhancement on computed tomography. *Eur J Radiol,* ***30:*** *206-213.*
9. Koike N, Cho A, Nasu K, Seto K, Nagaya S, Ohshima Y, *et al.* (2009) Role of diffusion-weighted magnetic resonance imaging in the differential diagnosis of focal hepatic lesions. *World J Gastroenterol,* ***15:*** *5805-5812.*
10. Bipat S, van Leeuwen MS, Comans EF, Pijl ME, Bossuyt PM, Zwinderman AH, *et al.* (2005) Colorectal liver metastases: CT, MR imaging, and PET for diagnosis--meta-analysis. *Radiology,* ***237:*** *123-131.*
11. Beyer T, Townsend DW, Brun T, Kinahan PE, Charron M, Roddy R, *et al.* (2000) A combined PET/CT scanner for clinical oncology. *J Nucl Med,* ***41:*** *1369-1379.*
12. Beyer T and Townsend DW (2006) Putting 'clear' into nuclear medicine: a decade of PET/CT development. *Eur J Nucl Med Mol Imaging,* ***33:*** *857-861.*
13. Poeppel TD, Krause BJ, Heusner TA, Boy C, Bockisch A, Antoch G (2009) PET/CT for the staging and follow-up of patients with malignancies. *Eur J Radiol,* ***70:*** *382-392.*
14. Veit-Haibach P, Luczak C, Wanke I, Fischer M, Egelhof T, Beyer T, *et al.* (2007) TNM staging with FDG-PET/CT in patients with primary head and neck cancer. *Eur J Nucl Med Mol Imaging,* ***34:*** *1953-1962.*
15. Veit-Haibach P, Kuehle CA, Beyer T, Stergar H, Kuehl H, Schmidt J, *et al.* (2006) Diagnostic accuracy of colorectal cancer staging with whole-body PET/CT colonography. *Jama,* ***296:*** *2590-2600.*
16. Antoch G, Stattaus J, Nemat AT, Marnitz S, Beyer T, Kuehl H, *et al.* (2003) Non-small cell lung cancer: dual-modality PET/CT in preoperative staging. *Radiology,* ***229:*** *526-533.*
17. Bolus NE, George R, Washington J, Newcomer BR (2009) PET/MRI: the blended-modality choice of the future? *J Nucl Med Technol,* ***37:*** *63-71; quiz 72-63.*
18. Wehrl HF, Judenhofer MS, Wiehr S, Pichler BJ (2009) Pre-clinical PET/MR: technological advances and new perspectives in biomedical research. *Eur J Nucl Med Mol Imaging, 36 Suppl* ***1:*** *S56-68.*
19. Antoch G and Bockisch A (2009)Combined PET/MRI: a new dimension in whole-body oncology imaging? *Eur J Nucl Med Mol Imaging, 36 Suppl* ***1:*** *S113-120.*
20. Seemann MD, Meisetschlaeger G, Gaa J, Rummeny EJ (2006) Assessment of the extent of metastases of gastrointestinal carcinoid tumors using whole-body PET, CT, MRI, PET/CT and PET/MRI. *Eur J Med Res,* ***11:*** *58-65.*
21. Donati OF, Hany TF, Reiner CS, von Schulthess GK, Marincek B, Seifert B, *et al.* (2010) Value of retrospective fusion of PET and MR images in detection of hepatic metastases: comparison with 18F-FDG PET/CT and Gd-

EOB-DTPA-enhanced MRI. *J Nucl Med,* ***51:*** *692-699.*
22. Antoch G, Kuehl H, Kanja J, Lauenstein TC, Schneemann H, Hauth E, *et al.* (2004) Dual-modality PET/CT scanning with negative oral contrast agent to avoid artifacts: introduction and evaluation. *Radiology,* ***230:****879-885.*
23. Beyer T, Antoch G, Blodgett T, Freudenberg LF, Akhurst T, Mueller S (2003) Dual-modality PET/CT imaging: the effect of respiratory motion on combined image quality in clinical oncology. *Eur J Nucl Med Mol Imaging,* ***30:*** *588-596.*
24. Carnaghi C, Tronconi MC, Rimassa L, Tondulli L, Zuradelli M, Rodari M, *et al.* (2007) Utility of 18F-FDG PET and contrast-enhanced CT scan in the assessment of residual liver metastasis from colorectal cancer following adjuvant chemotherapy. *Nucl Med Rev Cent East Eur,* ***10:****12-15.*
25. Zincirkeser S, Sahin E, Halac M, Sager S (2007) Standardized uptake values of normal organs on 18F-fluorodeoxyglucose positron emission tomography and computed tomography imaging. *J Int Med Res,* ***35:*** *231-236.*
26. Wiering B, Vogel WV, Ruers TJ, Oyen WJ (2008) Controversies in the management of colorectal liver metastases: role of PET and PET/CT. *Dig Surg,* ***25:*** *413-420.*
27. Small RM, Lubezky N, Shmueli E, Figer A, Aderka D, Nakache R, *et al.* (2009) Response to chemotherapy predicts survival following resection of hepatic colorectal metastases in patients treated with neoadjuvant therapy. *J Surg Oncol,* ***99:*** *93-98.*
28. Melton GB, Lavely WC, Jacene HA, Schulick RD, Choti MA, Wahl RL, *et al.* (2007) Efficacy of preoperative combined 18-fluorodeoxyglucose positron emission tomography and computed tomography for assessing primary rectal cancer response to neoadjuvant therapy. *J Gastrointest Surg,* ***11:*** *961-969; discussion 969.*